

Thermal Analysis of a piezo-disk ultrasound probe

Lorenzo Spicci, Marco Cati
Research and Development Department, Esaote S.p.A.
Via di Caciolle 15, 50127, Florence, Italy.
lorenzo.spicci@esaote.com, marco.cati@esaote.com

Abstract: Ultrasound imaging probes are widely used for several types of diagnosis applications. Since in most cases the duration of clinical examination can be quite long, the surface temperature of the probe head, in contact with human body, must be kept under control. International Safety Standard IEC 60601-2-37 sets an upper limit for the surface temperature in still air of 50°C (43°C if measured when coupled thermally and acoustically with a test object having thermal and acoustical properties mimicking those of an appropriate tissue).

The temperature rise is caused mainly by joule heating effect inside the active piezo-transducer and could be very important under some operating conditions (i.e. CW, Continuous Wave doppler; PW Pulsed Wave doppler; CFM, Colour Flow Mapping).

In the present work we focus our attention on a disk-type probe, which is widely used in CW and PW operating conditions. In particular we present a 2D-axial symmetry FEM for the probe, capable to predict both the operative temperature values at different driving signal frequencies, both the heating dynamics.

Moreover, the FEM is validated through comparison with specialized thermocouple surface temperature measurements. Finally a correlation between electric power and surface temperature is evaluated.

Keywords: thermal analysis, ultrasound transducer, piezoelectricity, FEM, COMSOL.

1. Introduction

Probes for diagnostic ultra-sonography application are devices that generate a pressure field into the human body, according to an electrical signal [1]. The efficiency of energy conversion, from applied electrical to stored mechanical one, is called (for a piezo-material) the *electromechanical coupling factor* k :

$$k^2 = \frac{\text{mechanical energy stored}}{\text{electric energy applied}} \quad (1)$$

Since k is always lower than 1, a temperature rise for the probe head occurs.

The main cause of the temperature rise are the joule losses in the piezo-transducer with the dynamics of heating controlled by specific heat and thermal conductivity values for the materials used in the probe construction and the final steady state temperature of the probe surface depending mainly on the internal loss of the piezo-material and the electrical driving power.

Since the probe head is kept in contact with the human body, the International Safety Standard IEC 60601-2-37 sets an upper limit for the surface temperature in still air of 50°C for whatever operating condition [2], in order to avoid skin burns or patient bother. In this sense, it's clear that a Finite Element Model (FEM) can greatly help in the study and optimization of the thermal behavior of the probe transducer.

In the present work, a disk-type probe (generally used for doppler examinations), operating in CW mode at 4 MHz central frequency and coupled in still air is designed and manufactured. The transducer design consists in a specialized piezo-material, a hard rubber backing substrate and one matching layer on top.

Thermal measurements are recorded on the top surface of the transducer using a k -type thermocouple and are compared with the FEM simulation results.

Finally, a theoretical model is presented, to show that it's possible to use a simplified equivalent circuit in order to estimate both the superficial temperature rise, both the specific thermal conductance of the transducer.

2. Multiphysics FEM

We briefly describe here the essential model characteristics that are used for the present COMSOL FEM.

The multi-physics approach is required because both the transducer and the surrounding fluid are modeled. In particular, the fluid (air) is modeled through “heat transfer” and “laminar flow” modules, while the piezo-disk transducer is modeled with the “piezo-electric” module.

2.1. Fluid modeling

The focus of our study is mainly the heating of the transducer due to its electrical losses, so we’re not going to report a complete theoretical background for the physics involved in the fluid heat transfer phenomena. For the reader interested in such theory, we suggest [3]. However, it’s worth to be noted that the *Boussinesq approximation* [4] is employed here for the fluid, as we’re interested only in convective flows around the transducer. In fact, for such condition the fluid flow can be considered as buoyancy-driven (also known as natural convection) and the density differences are sufficiently small to be neglected, except in gravitational terms in the heat equation [5]. The approximation makes the mathematics and physics simpler and can be easily introduced in the FEM as a volume force in the fluid domain surrounding the piezo-electric transducer.

2.2. Piezo-electric material modeling and electrical characteristics

The constitutive equations for a piezo-electric material are [6], in *stress-charge* form :

$$\begin{cases} \mathbf{T} = [\mathbf{c}^E] \mathbf{S} - [\mathbf{e}'] \mathbf{E} \\ \mathbf{D} = [\mathbf{e}] \mathbf{S} + [\boldsymbol{\epsilon}^S] \mathbf{E} \end{cases} \quad (2)$$

where \mathbf{T} is the stress vector, \mathbf{c} is the elasticity matrix, \mathbf{S} is the strain vector, \mathbf{e} is the piezo-electric matrix, \mathbf{E} is the electric field vector, \mathbf{D} is the electric displacement vector, $\boldsymbol{\epsilon}$ is the dielectric permittivity matrix. The superscripts indicate a zero or constant corresponding field.

Equations (2) takes into account both piezo-electricity, both mechanical and electrical anisotropy of the material.

From the electrical point of view, the electrical impedance Z of a piezo-electric disk can be calculated from the potential difference V and the flowing current I across the disk faces. V is impressed between the disk faces, while I is calculated as surface integral of the current density component along z -axis.

Moreover, the electrical conductivity and dielectric losses are specified for the piezo-material, so that the resulting heating effects are recalled in the fluid as a power dissipation source.

3. Study layout

The study progressed as follows:

- 1) Manufacturing of the specialized piezo-disk transducer (§3.1).
- 2) Developing of the corresponding COMSOL FEM to simulate the worst case heating configuration for the piezo-disk (§3.2).
- 3) Design of an electrical circuit model (§3.4).
- 4) Comparison between measurements and FEM simulations, along with electrical circuit analysis results, in order to validate the COMSOL FEM (§4).

The thermal heating measurements of the top surface were performed with thermocouple equipment (§3.3).

3.1. Transducer manufacturing

The piezo-electric disk transducer was built with top quality manufacturing procedures, in order to have the best comparison with model simulation (Figure 1).

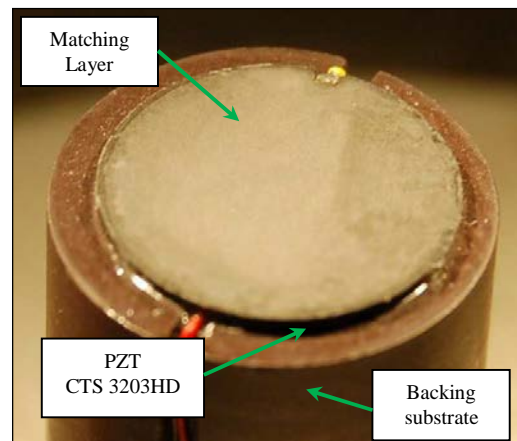


Figure 1: Disk-type piezo-transducer assembly.

In order to work as a PW or CW transducer, the piezo-electric material needs to be bond on a backing substrate material which acts not only as a support, but also as an efficient damper for the back-traveling pressure wave: a high density (3700 g/cm^3) rubber was chosen.

On the other hand, a tungsten-powder-loaded epoxy was bond in front of the ceramic, acting as

acoustic impedance matching layer, between high impedance ceramic (30-35 MRayls) and low impedance acoustic medium (i.e. human tissue, ~ 1.5 MRayls).

These two materials are modeled in COMSOL by entering the Young modulus, Poisson ratio and density respective values.

3.2. Building the COMSOL model

The FEM for the transducer array was built using the COMSOL *piezo-electric* module, along with *laminar flow* and *heat transfer* modules, in 2D axial symmetry space dimension. Mesh on all domains was chosen as free tetrahedral and boundary layers were employed on the transducer-fluid contact surface (Figure 2).

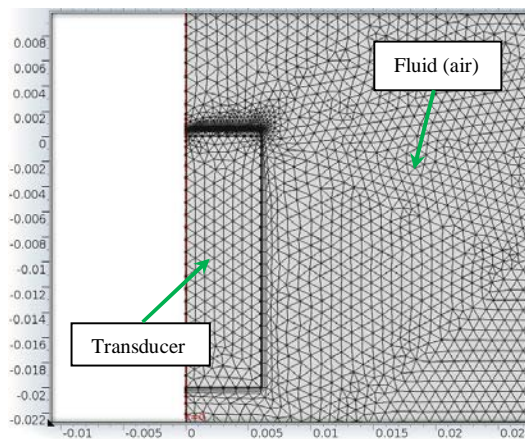


Figure 2: Transducer 2D-axial symmetry FEM.

3.3. Measurement equipment

The transducer's basic performances can be evaluated by measurement of the electrical impedance; whose quality and reliability play an important role in the comparison with simulation results. For a complete transducer-performance analysis and optimization, we invite the reader to look at our previous work [7]. Here, in section §4, we report the final electrical impedance comparison between measurements, performed with Hewlett Packard 4195A Network Analyzer, and optimized FEM results.

As regard temperature measurements, the piezo-disk transducer was powered with Agilent 33250A Function Generator instead of an Esaote scanner device, since the equipment is easier to manage and practically equivalent: 1) internal impedance is 50Ω , quite close to the actual ultrasound scanner driving circuit impedance

and, 2) the driven signal was set to a sinusoidal CW with the same RMS value¹ and frequency of the worst case operating condition experienced during clinical examination (open circuit V_0 voltage of 7 V RMS, i.e. about 10 V peak amplitude, see §3.4).

Moreover, we make use of a micro-voltmeter with type *k* thermocouple (Figure 3), applied to the transducer surface. The thermocouple head was coupled to the piezo-disk surface with thermal paste and the head dimensions was chosen to be less than 1 mm in order to get a negligible inertial thermal effect. Note that the *k* type thermocouple sensitivity of about $41 \mu\text{V}/^\circ\text{C}$ is capable to describe with high accuracy also a very low thermal variation of the disk-probe.

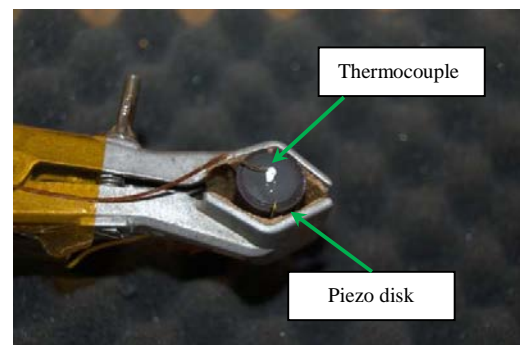


Figure 3: *k* type thermocouple measurement.

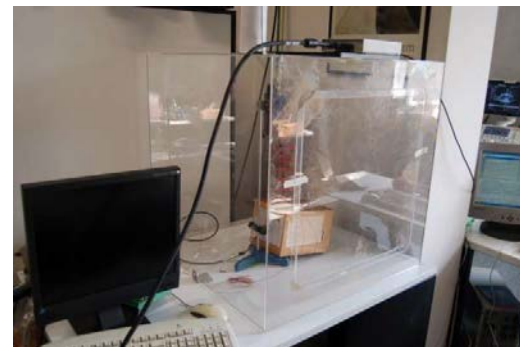


Figure 4: Plexiglass box for thermal measurements.

Thermal measurements were performed in a thermostatic environment at 28°C using a specialized plexiglass box in order to avoid any additional and uncontrolled convective flux (Figure 4).

¹ The RMS value of an alternating current is also known as its *heating value*, as it is a voltage which is equivalent to the direct current value that would be required to get the same heating effect.

Using the above set-up the uncertainty of the temperature measurement can be evaluated in $\pm 2^\circ\text{C}$.

3.4. Piezo-transducer equivalent circuit and dissipated power

A piezo-electric transducer can be modeled by the well known KLM model [8] that is able to depicts both its electrical and mechanical characteristics. For a thermal analysis, we can consider the impedance $Z(f) = Z_{KLM}$ as representative of the electrical behavior of the transducer. Figure 5 reports the electrical circuit model of the piezo-electric transducer along with the function generation and its internal impedance, $R = 50\Omega$.

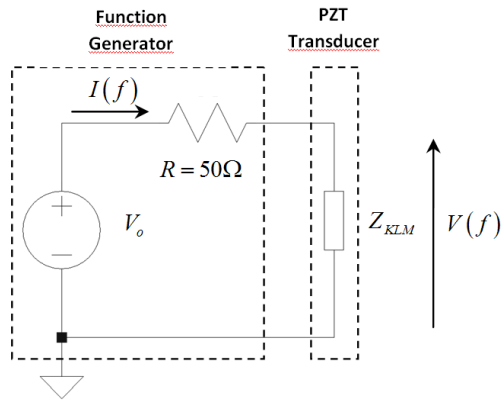


Figure 5: Piezo-transducer equivalent circuit.

If $I(f)$ is the total current that flows into the piezo-transducer at the frequency f , the power dissipated due to joule effect is expressed by:

$$P(f) = \text{Re}\{Z(f)\} |I(f)|^2 \quad (3)$$

Where $\text{Re}\{Z(f)\}$ is the real part of the impedance $Z(f)$. If $V(f)$ is the voltage across the piezo-transducer, the current $I(f)$ can be expressed by:

$$I(f) = \frac{V(f)}{Z(f)} \quad (4)$$

Substituting (4) into (3) we finally obtain:

$$P(f) = \text{Re}\{Z(f)\} \left| \frac{V(f)}{Z(f)} \right|^2 \quad (5)$$

Comparing the dependency of power and temperature on frequency, it's possible to verify

a direct correspondence and define a *heat transfer coefficient* "h" as follows:

$$h = \frac{P}{S \cdot \Delta T} \quad (6)$$

Where P is the dissipated power, S is the heat transfer surface area and ΔT is the difference in temperature between the solid surface and the fluid in contact.

The result of this calculation will be shown in §4, reporting the study and measurement results.

4. Results

We present here the results obtained from the FEM, along with the corresponding measurements and their comparison with the equivalent circuit model.

4.1. Electric Impedance Piezo-electric plate

The piezo-electric material chosen for the ultrasound disk transducer is a standard piezo-ceramic CTS 3203HD [9], having a diameter of 12 mm and thickness of 0.5 mm. The value of resonance frequency for the first thickness mode of vibration is about 4 MHz.

As reported before, the piezo-disk is stuck on a backing material cylinder and an acoustic matching layer is glued on top. These two isotropic elastic materials have an important effect on the transducer resulting electric impedance.

Due to the large number of parameters to be determined, we decided to follow a *step approach* procedure, that consists in the following steps of analysis:

- 1) Simulation and measurements for the piezo-ceramic disk alone.
- 2) Simulation and measurements for the piezo-ceramic disk bonded on backing substrate.
- 3) Simulation and measurements for the complete transducer (piezo-ceramic disk, backing substrate and front matching layer).

For each of the step above, the optimization is based on root mean square minimization for the objective function given by the difference between measured and simulated electrical impedance, from a frequency analysis simulation. The results of such analysis are reported in our previous work [7].

Here we report (Figure 6) the final result, which shows good agreement between simulation and measurements. In particular, resonance and anti-resonance frequency fit error is less that 5%.

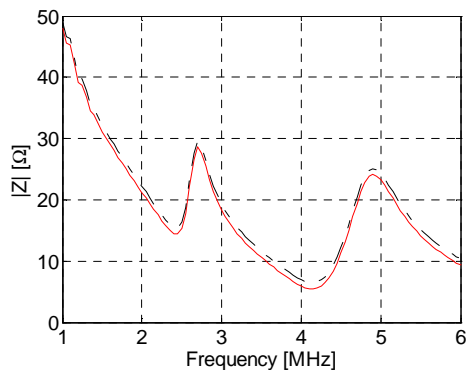


Figure 6: Piezo-disk complete transducer electrical impedance magnitude. Comparison between simulations (solid) and measurements (dashed).

Moreover, both resonance due to piezo-ceramic (~4 MHz) and resonance due to matching layer (~2.4 MHz) are clearly visible.

4.2. Temperature rise of front face

After the transducer is analyzed in terms of electrical impedance, we can focus on the temperature rise of the front face (in contact with the patient). In order to validate the model, we start comparing the results from measurements and simulations, considering a driving sinusoidal voltage amplitude corresponding to the “worst heating case” configuration and an environment temperature of 28 °C.

The most interesting analysis is a frequency sweep that points out which frequency (between 2 MHz and 6 MHz operative range) leads to maximum heating of the transducer front face (Figure 7).

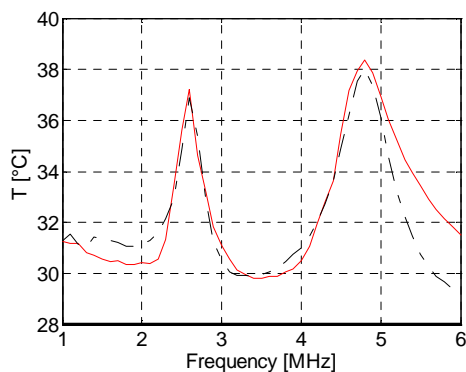


Figure 7: Transducer front face equilibrium temperature, dependency on frequency. Comparison between simulations (solid) and measurements (dashed). Environment temperature: 28°C.

Agreement between measurement and simulation results is good, within an error of about 1°C for final equilibrium temperature.

It’s very interesting to note the large variation of final equilibrium temperature between resonance and anti-resonance operating frequencies of the piezo-disk transducer. It’s clear that heating is maximum at anti-resonance frequencies (where the value of electrical impedance is maximum) and minimum close to resonance frequencies (where the value of electrical impedance is minimum). Finally, even at 4.8 MHz, where the temperature value is maximum, the limit of 50°C is not reached.

It’s important to compare the temperature behavior reported in Figure 7 with the dissipated power calculated with (5), using the measured values for electrical impedance $Z(f)$ and driving voltage $V(f)$ (Figure 8).

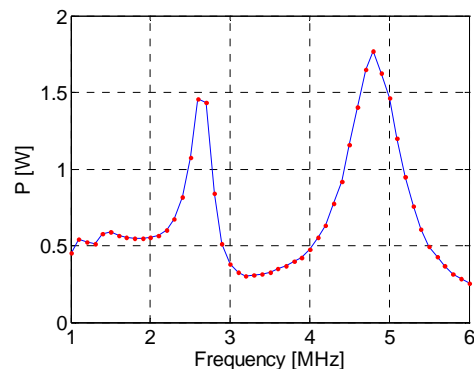


Figure 8: Dissipated power (calculated from equivalent circuit) versus frequency.

The correlation between Figure 8 and Figure 7 is evident so that, starting from (6), it’s interesting to depict (Figure 9) the measured *specific thermal conductance* defined as the product by the *heat transfer coefficient* “h” by the disk surface S of the transducer. The frequency behavior of the specific thermal conductance for the manufactured disk-type transducer is approximately constant over the overall frequency range with mean value of 0.17 W/°C (solid red line) and with a standard deviation of 6.8% (dashed red line).

Moreover, in Figure 10 it’s reported the heating transient behaviour, referring to the piezo-disk principal resonance (4 MHz) and anti-resonance frequencies (4.8 MHz).

Again, agreement between simulation results and measurements can be considered good, both in term of stationary final temperature (error less than 1°C) and in term of heating transient time constant. Such agreement can be also used to predict the time interval that the system takes to reach a given temperature value.

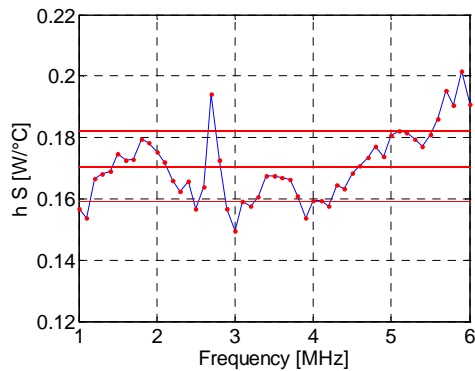


Figure 9: Piezo-disk transducer measured specific thermal conductance ($h \cdot S$) versus frequency.

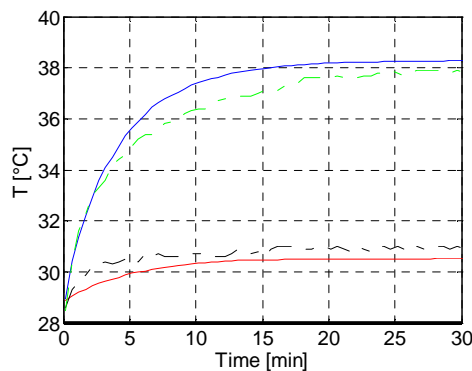


Figure 10: Transducer front face temperature rise at 4 MHz (resonance) and 4.8 MHz (anti-resonance). Comparison between simulations (solid) and measurements (dashed). Environment temperature: 28°C.

Finally, as regard the analysis of the cooling fluid around the transducer (air), a 2D axial symmetry color temperature and field velocity map for the fluid is shown in Figure 11, for a CW excitation signal at 4 MHz.

From Figure 11 we note that the transversal section of the fluid subjected to some heating effect is limited to some millimeters around the lateral surface of the piezo-disk transducer.

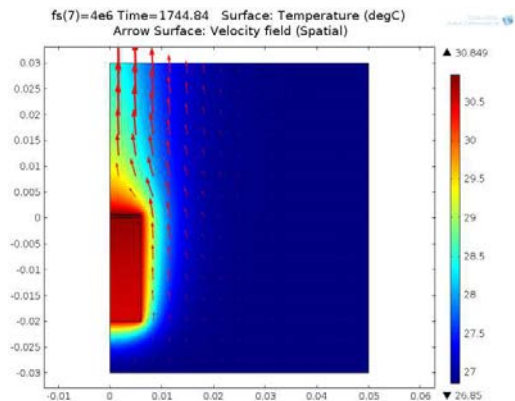


Figure 11: Fluid (air) temperature and velocity map at 4 MHz excitation frequency (resonance). Environment temperature: 28°C.

5. Conclusions and future work

A FEM model has been developed and validated to study the heating of an ultrasound piezo-disk transducer, operating in CW mode and coupled in still air, in order to verify if the upper limit for the surface temperature imposed by International Safety Standard EN 61000-2-37 is fulfilled.

Such limit of 50°C in still air and 43°C if the transducer is coupled with a test object mimicking appropriate tissue, is important in order to avoid skin burns or patient bother.

Frequency analysis and transient simulations show a good agreement between measured and simulated performances both in term of stationary final temperature (error less than 1°C) and in term of heating transient time constant.

The temperature rise is found to be larger at anti-resonance with respect to resonance frequencies, suggesting that the absorbed input power is larger.

Finally, the theoretical model presented shows that it is possible to use a simplified equivalent circuit in order to estimate both the superficial temperature rise, both the specific thermal conductance of the transducer, with an error of less than 10%.

6. Acknowledgment

The authors would like to thank Dr. Michele Bassani of Esaote S.p.A. and Dr. Michele Piccinno of Dipartimento di Fisica “Enrico Fermi” of Università di Pisa for their constructive criticism and suggestions.

7. References

- [1] P. Fish, "Physics and Instrumentation of Diagnostic Medical Ultrasound", Wiley, June 1990.
- [2] IEC 60601-2-37, "*Medical electrical equipment - part 2: particular requirements for the safety of ultrasonic medical diagnostic and monitoring equipment*".
- [3] G. K. Batchelor, "*An Introduction to Fluid Dynamics*", Cambridge University Press, 1972, ISBN 0-521-66396-2.
- [4] J. Boussinesq, "*Théorie de l'écoulement tourbillonnant et tumultueux des liquides dans les lits rectilignes a grande section*", Paris, Gauthier-Villars et fils, 1897.
- [5] D. H. Peregrine, "*Equations for water waves and the approximations behind them*", Ed. R.E. Meyer., 1972, Waves on Beaches and Resulting Sediment Transport., Academic Press. pp.95–122. ISBN 0-12-493250-9.
- [6] COMSOL Multiphysics Acoustic Module User Guide, ver.3.5a, pages 32-33.
- [7] L. Spicci, M. Cati, "*Ultrasound Piezodisk Transducer Model for Material Parameter Optimization*", Comsol Conference 2010, Paris (best paper award).
- [8] R. Krimholtz, D. A. Leedom, G.L.Matthei, "*New equivalent circuits for elementary piezoelectric transducers*", Electron. Lett., vol. 6, pp. 398–399, June 1970.
- [9] S. Sherrit, *et alii*, "*A complete characterization of the piezoelectric, dielectric, and elastic properties of Motorola PZT 3203 HD including losses and dispersion*", SPIE, Vol. 3037, Feb 1997.